

Extensive sampling of basidiomycete genomes demonstrates inadequacy of the white-rot/brown-rot paradigm for wood decay fungi

Robert Riley^a, Asaf A. Salamov^a, Daren W. Brown^b, Laszlo G. Nagy^c, Dimitrios Floudas^c, Benjamin W. Held^d, Anthony Levasseur^e, Vincent Lombard^f, Emmanuelle Morin^g, Robert Otillar^a, Erika A. Lindquist^a, Hui Sun^a, Kurt M. LaButti^a, Jeremy Schmutz^{a,h}, Dina Jabbourⁱ, Hong Luoⁱ, Scott E. Baker^j, Antonio G. Pisabarro^k, Jonathan D. Waltonⁱ, Robert A. Blanchette^d, Bernard Henrissat^f, Francis Martin^g, Dan Cullen^l, David S. Hibbett^{c,1}, and Igor V. Grigoriev^{a,1}

^aUS Department of Energy (DOE) Joint Genome Institute, Walnut Creek, CA 94598; ^bUS Department of Agriculture (USDA), Peoria, IL 61604; ^cDepartment of Biology, Clark University, Worcester, MA 01610; ^dUniversity of Minnesota, St. Paul, MN 55108; ^eInstitut National de la Recherche Agronomique, Unité Mixte de Recherche 1163, Aix-Marseille Université, 13288 Marseille, France; ^fCentre National de la Recherche Scientifique, Unité Mixte de Recherche 7257, Aix-Marseille Université, 13288 Marseille, France; ^gInstitut National de la Recherche Agronomique, Unité Mixte de Recherche 1136, Institut National de la Recherche Agronomique-Université de Lorraine, Interactions Arbres/Micro-organismes, 54280 Champenoux, France; ^hHudsonAlpha Institute of Biotechnology, Huntsville, AL 35806; ⁱDOE Great Lakes Bioenergy Research Center, Michigan State University, East Lansing, MI 48824; ^jEnvironmental Molecular Sciences Laboratory, Pacific Northwest National Laboratory, Richland, WA 99354; ^kDepartamento de Producción Agraria, Universidad Pública de Navarra, 31006 Pamplona, Spain; and ^lUSDA Forest Products Laboratory, Madison, WI 53726

Edited* by Thomas N. Taylor, University of Kansas, Lawrence, KS, and approved May 16, 2014 (received for review January 12, 2014)

Basidiomycota (basidiomycetes) make up 32% of the described fungi and include most wood-decaying species, as well as pathogens and mutualistic symbionts. Wood-decaying basidiomycetes have typically been classified as either white rot or brown rot, based on the ability (in white rot only) to degrade lignin along with cellulose and hemicellulose. Prior genomic comparisons suggested that the two decay modes can be distinguished based on the presence or absence of ligninolytic class II peroxidases (PODs), as well as the abundance of enzymes acting directly on crystalline cellulose (reduced in brown rot). To assess the generality of the white-rot/brown-rot classification paradigm, we compared the genomes of 33 basidiomycetes, including four newly sequenced wood decayers, and performed phylogenetically informed principal-components analysis (PCA) of a broad range of gene families encoding plant biomass-degrading enzymes. The newly sequenced *Botryobasidium botryosum* and *Jaapia argillacea* genomes lack PODs but possess diverse enzymes acting on crystalline cellulose, and they group close to the model white-rot species *Phanerochaete chrysosporium* in the PCA. Furthermore, laboratory assays showed that both *B. botryosum* and *J. argillacea* can degrade all polymeric components of woody plant cell walls, a characteristic of white rot. We also found expansions in reducing polyketide synthase genes specific to the brown-rot fungi. Our results suggest a continuum rather than a dichotomy between the white-rot and brown-rot modes of wood decay. A more nuanced categorization of rot types is needed, based on an improved understanding of the genomics and biochemistry of wood decay.

lignocellulose | phylogenomics | bioenergy

Fungi of the phylum Basidiomycota (basidiomycetes) comprise 32% of the described fungi (1) and are important to forestry (2–4), agriculture (5–7), and medicine (8–11). This diverse phylum includes the mushrooms (12–14); pathogens of plants (2), animals (9–11), and other fungi (15); osmotically tolerant molds (16); ectomycorrhizal symbionts like *Laccaria bicolor*, which are critical for plant growth; plant pathogens, such as rusts and smuts (7); and saprotrophs, including wood-decaying fungi (17).

The 26,000 basidiomycete taxa in the National Center for Biotechnology Information (NCBI) database (18, 19) are divided into three subphyla: Agaricomycotina (~22,000 taxa), Pucciniomycotina (~2,300 taxa), and Ustilaginomycotina (~1,000 taxa). Agaricomycotina includes many decomposers of wood and leaf litter (12, 17, 20–23) that produce lignocellulolytic enzymes that

have potential to be used in bioenergy production (24–27). Thus, much of sequencing effort at the US Department of Energy (DOE) Joint Genome Institute (JGI) (<http://jgi.doe.gov/fungi>) has targeted Agaricomycotina, particularly the Agaricomycetes (mushroom-forming fungi), with the large orders Agaricales (predominantly gilled mushrooms), Polyporales (wood-decaying polypores and others), and Boletales (porcini mushrooms and others) being especially deeply sampled.

A keen focus in the comparative genomics of Basidiomycota has concerned lineages of wood decay fungi (13, 17, 20–23, 28). For decades, two broad categories have been recognized: white rot and brown rot (29–31). During brown rot, cellulose is rapidly

Significance

Wood decay fungi have historically been characterized as either white rot, which degrade all components of plant cell walls, including lignin, or brown rot, which leave lignin largely intact. Genomic analyses have shown that white-rot species possess multiple lignin-degrading peroxidases (PODs) and expanded suites of enzymes attacking crystalline cellulose. To test the adequacy of the white/brown-rot categories, we analyzed 33 fungal genomes. Some species lack PODs, and thus resemble brown-rot fungi, but possess the cellulose-degrading apparatus typical of white-rot fungi. Moreover, they appear to degrade lignin, based on decay analyses on wood wafers. Our results indicate that the prevailing paradigm of white rot vs. brown rot does not capture the diversity of fungal wood decay mechanisms.

Author contributions: R.R., S.E.B., A.G.P., J.D.W., R.A.B., B.H., F.M., D.C., D.S.H., and I.V.G. designed research; R.R., D.W.B., L.G.N., D.F., B.W.H., A.L., E.M., and R.A.B. performed research; A.G.P., J.D.W., B.H., and D.S.H. contributed new reagents/analytic tools; R.R., A.A.S., D.W.B., L.G.N., D.F., A.L., V.L., E.M., R.O., E.A.L., H.S., K.M.L., J.S., D.J., and H.L. analyzed data; and R.R., D.W.B., J.D.W., R.A.B., B.H., D.C., D.S.H., and I.V.G. wrote the paper.

The authors declare no conflict of interest.

*This Direct Submission article had a prearranged editor.

Freely available online through the PNAS open access option.

Data deposition: The sequences reported in this paper have been deposited in the GenBank database [AYEP0000000 (*Botryobasidium botryosum*), AYUM0000000 (*Galerina marginata*), AYUL0000000 (*Jaapia argillacea*), and AYUK0000000 (*Pleurotus ostreatus*)].

¹To whom correspondence may be addressed. E-mail: IVGrigoriev@lbl.gov or dhibbett@clarku.edu.

This article contains supporting information online at www.pnas.org/lookup/suppl/doi:10.1073/pnas.1400592111/-DCSupplemental.

depolymerized via oxidative mechanisms, whereas modified lignin remains as a polymeric residue (32–35). In contrast, white-rot fungi use hydrolases that gradually degrade cellulose while lignin is completely mineralized. Lignin degradation involves high-oxidation potential class II peroxidases (PODs) that, on the basis of conserved catalytic and Mn-binding sites, are classified as lignin peroxidase (LiP), manganese peroxidase (MnP), or versatile peroxidase (VP) (36–38). The first genomes of the white-rot fungus *Phanerochaete chrysosporium* and brown-rot fungus *Postia placenta* revealed a gene complement consistent with their respective modes of wood decay (22, 23). Further comparative genomics studies of larger sets of wood decay fungi supported a consistent relationship between decay patterns and several enzyme families. Specifically, white-rot fungi had high-oxidation potential PODs for lignin degradation as well as cellobiohydrolases for degrading crystalline cellulose. Classified in glycoside hydrolase (GH) families (39) GH6 and GH7, cellobiohydrolases attack cellulose in a synergistic manner and often carry a cellulose binding module (CBM1). In contrast, the genomes of brown-rot fungi did not encode PODs and the predicted cellobiohydrolase-encoding genes were generally absent or lacking a CBM1 domain.

Here, we present comparative analyses of 33 sequenced basidiomycete genomes (Table S1). Included are 22 wood decayers, of which *Galerina marginata*, *Pleurotus ostreatus*, *Botryobasidium botryosum*, and *Jaapia argillacea* are newly sequenced. The results call into question the prevailing white-rot/brown-rot dichotomy.

Results and Discussion

Phylogeny and Protein Conservation. A maximum-likelihood (ML) phylogeny (40) was inferred from protein sequence alignments of 183 conserved gene families (Fig. S14). Overall, the tree topology is consistent with prior studies using genome-scale datasets (17) as well as phylogenetic analyses using small numbers of genes (41), such as the sister group relationship between Ustilaginomycotina and Agaricomycotina, and the placement of *Wallemia sebi* (Wallemiomycetes) as the sister group of the rest of the Agaricomycotina (16). Brown-rot fungi are polyphyletic, as shown previously (17), and include species in Polyporales, Boletales, Gloeophyllales, and Dacrymycetales. Some aspects of the phylogeny remain uncertain: our placement of *Jaapia argillacea* as the sister group of the Gloeophyllales conflicts with a previous study using six genes (42); and *Auricularia delicata* was inferred as the sister group of *Piriformospora indica*, differing from multigene phylogenies (41, 43–45), which suggested that these lineages form a paraphyletic assemblage.

Gene families in 33 basidiomycetes and 30 other fungi (Table S2) with sequenced genomes were inferred by Markov chain (MCL) clustering (46) of all-vs.-all protein BLAST (47) alignments. Analysis of protein conservation suggests a conserved core fungal genome of ~5,000 genes (Fig. S1C). Roughly one-half of the proteins (49%) in Basidiomycota lack homologs in other groups of fungi, and 23% of Basidiomycota proteins are unique to a single organism (i.e., each of the 33 basidiomycetes analyzed harbored proteins not found in any other sampled species, ranging from 4% to 51%). In contrast, in Ascomycota, 30% of the proteins are phylum specific and 13% are organism specific (using a comparative set of 27 Ascomycota fungi; Table S2). We were able to assign functions from the Eukaryotic Clusters of Orthologs (KOG) (48) to 38% of Basidiomycota proteins (compared with 43% in Ascomycota); 74% of core proteins in both Basidiomycota and Ascomycota; and 17% of Basidiomycota-specific proteins (23% in Ascomycota) (Fig. S2).

Diversity of CAZymes and Associated Activities in Basidiomycota. Thirty-three basidiomycete genomes were searched for genes whose protein products are implicated in the breakdown of the polysaccharide portion of plant cell walls (cellulose, hemicellulose, pectin) using the CAZy database pipeline (39, 49). The

number of genes in each CAZy family, in each organism, is presented in Dataset S1.

Cellulolytic families. During white-rot decay, cellulose is targeted primarily by hydrolytic enzymes of multiple GH families. Lytic polysaccharide monoxygenases (LPMOs) of the AA9 family (formerly GH61) also participate via oxidative mechanisms. White-rot fungi generally have more cellulolytic genes (both hydrolytic and oxidative) and cellulose binding domains (CBM1) relative to brown-rot fungi (Fig. 1). Cellobiohydrolases of families GH6 and GH7 (which cleave cellulose to the disaccharide cellobiose) are correlated with white rot [$r = 0.3$ and 0.6 , respectively, by the independent contrasts method (50)]. Likely involved in boosting cellulase activity (51–54), LPMOs are abundant in white-rot fungi ($r = 0.3$) but reduced in brown-rot fungi ($r = -0.5$). Cellobiose dehydrogenases (family AA3_1), which enhance cellulose degradation (52), are uniformly present in a single copy in all white-rot fungi and absent from the majority of brown-rot fungi (although *Gloeophyllum trabeum* has one copy, and Boletales *Coniophora puteana* and *Serpula lacrymans* each have two copies). Additional cellulolytic families were found in basidiomycetes. For examples, GH5 (containing endo-acting cellulases as well as many other enzymes of differing substrate specificity; Dataset S2), GH12, GH44, and GH45 are expanded in white-rot fungi ($r = 0.2, 0.1, 0.4, 0.5$, respectively) and diminished in brown-rot fungi ($r < -0.2$; for all, see also Dataset S1).

Among the newly sequenced genomes, *G. marginata*, *P. ostreatus*, *B. botryosum*, and *J. argillacea* all possess diverse CAZymes typical of white-rot fungi. *B. botryosum* has 32 genes encoding LPMOs, and three encoding cellobiose dehydrogenases, both more than any other wood decay fungus in our set. *J. argillacea* has 15 genes encoding LPMOs, and one encoding a cellobiose dehydrogenase, both numbers typical of white-rot fungi. A similar pattern is evident when considering families GH6, GH7, and CBM1; *B. botryosum* and *J. argillacea* show a genetic complement similar to white-rot fungi.

Hemicellulolytic and pectinolytic families. Hemicellulose and pectin comprise a variety of linear and branched complex polysaccharides. Hemicellulose includes xylans, xyloglucans, glucuronoxylans, arabinoxylans, mannans, glucomannans, and galactoglucomannans. Pectins include polygalacturonic acid, linear and branched rhamnogalacturonans, and arabinogalactans. Basidiomycetes contain some seven CAZy families that target hemicelluloses, and 11 that target pectins (Table S3). In contrast to the cellulolytic families, there is not a clear dichotomy in which white-rot fungi have more genes encoding hemicellulases and pectinases, and brown-rot fungi have fewer (Dataset S1).

Distribution of Lignin-Degrading Enzymes Blurs the Distinction Between White- and Brown-Rot Fungi. With respect to PODs, there was a clear dichotomy between white-rot fungi, which have various combinations of MnP, LiP, and VP ($r = 0.8$), and brown-rot fungi, which lack PODs ($r = -0.5$). By this measure, the newly sequenced *G. marginata* and *P. ostreatus* resemble typical white-rot fungi with 10 and 9 PODs, respectively. In contrast, *B. botryosum* and *J. argillacea* resemble typical brown-rot fungi in their lack of PODs. *Schizophyllum commune* had previously been characterized as a white-rot fungus (55), but it also lacks PODs. The one class II peroxidase in *J. argillacea* lacks the catalytic Trp and Mn-binding sites, and is therefore classified as a generic peroxidase (56, 57) that is unlikely to directly modify lignin. Affirming the observed genetic complement, extracellular filtrates from *J. argillacea* and *B. botryosum* cultures were unable to oxidize veratryl alcohol or 2,6-dimethoxyphenol, standard substrates for high-oxidation potential PODs (58, 59). According to our phylogeny (Fig. S14), the contraction of ligninolytic PODs in *J. argillacea* may have arisen before its evolutionary separation from *G. trabeum* because both species lack these proteins. However, *G. trabeum* also has a reduced complement of

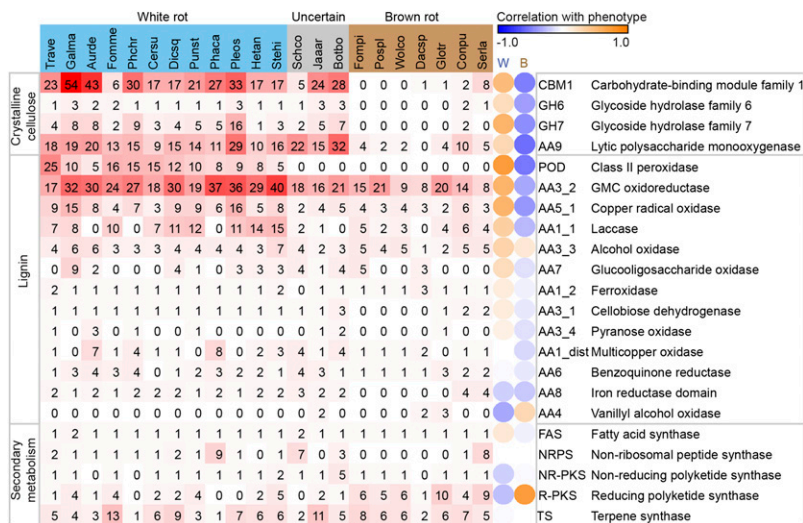


Fig. 1. Lignocellulose-degrading and secondary metabolism in wood-decaying fungi. Organisms use the following abbreviations: Aurde, *Auricularia delicata*; Botbo, *Botryobasidium botryosum*; Cersu, *Ceriporiopsis subvermisporea*; Conpu, *Coniophora puteana*; Dacsp, *Dacryopinax* sp.; Dicsq, *Dichomitus squalens*; Fomme, *Fomitiporia mediterranea*; Fompi, *Fomitopsis pinicola*; Galma, *Galerina marginata*; Glotr, *Gloeophyllum trabeum*; Hetan, *Heterobasidion annosum*; Jaaar, *Jaapia argillacea*; Phaca, *Phanerochaete carnosae*; Phchr, *Phanerochaete chrysosporium*; Pleos, *Pleurotus ostreatus*; Pospl, *Postia placenta*; Punst, *Punctularia strigosozonata*; Schco, *Schizophyllum commune*; Serla, *Serpula lacrymans*; Stehi, *Stereum hirsutum*; Trave, *Trametes versicolor*; Wolco, *Wolfiporia cocos*. Gene number is shaded red/white, and independent-contrasts correlation of enzyme with rot type is shaded orange/blue. Notice a strict white/brown-rot dichotomy with respect to the lignin-attacking PODs and the CAZymes that target crystalline cellulose (CBM1, GH6, and GH7), and a continuum with other lignin-targeting enzymes.

enzymes attacking crystalline cellulose and is a model system for brown rot (60, 61).

Although PODs have been shown to be important for lignin degradation, numerous other classes of enzymes are capable of degrading, or at least modifying, lignin and about a dozen kinds of enzymes potentially participating in ligninolysis are found in basidiomycetes (Fig. 1). The multicopper oxidases of family AA1 are such an example. Laccases (subfamily AA1_1) may be capable of cleaving lignin bonds in the presence of certain mediators (62) and are more abundant in white-rot fungi than brown-rot fungi (Fig. 1; $r = 0.4$ for white rot; $r = -0.3$ for brown rot). In the cases of *J. argillacea* and *B. botryosum*, no laccase activity was detected in concentrated culture filtrates (63). Nevertheless, the white-rot fungi *P. chrysosporium*, *Phanerochaete carnosae*, and *A. delicata* have no basidiomycete-type laccases *sensu stricto* (17). These three fungi instead have four to eight genes each of the related AA1_dist subfamily of multicopper oxidases (which, predictably, are reduced in brown-rot fungi at 0 to two genes), reflecting the diversity of chemistries used in lignin degradation.

Correlations Between Decay Mode and Secondary Metabolism. Secondary metabolites include polyketides, nonribosomal peptides, and terpenoids, among many other substances that are not considered to be critically involved in an organism's growth, development, and reproduction, but that typically confer some advantage in the never-ending competition with other organisms (64). To assess the diversity of secondary metabolism in basidiomycetes, we characterized fatty acid synthases (FASs), non-ribosomal peptide synthases (NRPSs), polyketide synthases (PKSs), and terpene synthases (TSs). PKSs were additionally subdivided into reducing and nonreducing (R-PKS and NR-PKS), each of which was further divided into subfamilies (Fig. S3). Secondary metabolism enzymes are summarized in the lower panel of Fig. 1.

Wood-decaying basidiomycetes tend to have similar numbers of FAS and NR-PKS genes (approximately one gene each), with the exception of *B. botryosum*, which has five NR-PKS genes. NRPSs vary in gene number (0 to nine genes), with no apparent correlation with lifestyle. TS genes, as well, vary in number (1–13 genes), with no apparent lifestyle correlation.

R-PKSs are expanded in the brown-rot fungi, with all but the phylogenetically basal *Dacryopinax* sp. possessing 4–14 R-PKS genes. In contrast, the white-rot fungi have generally fewer R-PKS genes and many taxa lack them entirely. R-PKS gene number correlates with brown rot (independent-contrasts $r = 0.8$). Although it was previously suggested that secondary

metabolism could play a role in wood decay by the brown-rot fungus *Serpula lacrymans* (20), a widespread pattern of secondary metabolism expansion has not yet been reported for brown-rot fungi in general. The observation that the number of R-PKS genes is expanded in three phylogenetically distinct clades of brown-rot fungi: the Boletales (*S. lacrymans* and *C. puteana*), the Polyporales (*Wolfiporia cocos*, *P. placenta*, and *Fomitopsis pinicola*), and Gloeophyllales (*G. trabeum*), suggests that R-PKSs have a possible role in the brown-rot lifestyle, and that the apparent correlation is not an artifact of phylogenetic sampling. The exact biochemical role of R-PKSs in wood rot in general is unknown. However, it has been suggested that secondary metabolites including certain catechols and quinones can serve as extracellular Fe^{3+} reductants in *G. trabeum*, *S. lacrymans*, *P. placenta*, and *W. cocos*. Together with H_2O_2 , the reduced iron is thought to drive a nonenzymatic Fenton reaction in which highly reactive hydroxyl radicals depolymerize cellulose (20, 65–68).

Secondary metabolism plays a critical role for fungal survival and success, including Basidiomycota (69), and a rich array of secondary metabolism genes has been reported in *Serpula lacrymans* and *Postia placenta* (20), and *Omphalotus olearius* (70). It may be that secondary metabolites, widely considered to confer advantage by inhibiting competing microorganisms, are more important in the ecological niches occupied by brown-rot fungi, compared with white-rot fungi. Indeed, our observation that expansions of R-PKSs are correlated with brown rot in multiple polyphyletic lineages highlights gaps in our knowledge of the mechanisms of wood decay even in well-studied species of Boletales, Polyporales, and Gloeophyllales.

Insights into Diversity of Decay Mechanisms from Phylogenetically Informed Principal-Components Analyses of Decay-Related Gene Families. The expanded sampling of basidiomycete genomes presented here includes species (*B. botryosum*, *J. argillacea*, and *S. commune*) that deviate from the classical models of white rot vs. brown rot, in that they lack PODs (like brown-rot fungi) but possess diverse arrays of enzymes acting on crystalline cellulose (like white-rot fungi). To visualize the diversity of decay chemistries in basidiomycetes, we applied phylogenetically informed principal-components analysis (PCA) (71) to the set of predicted carbohydrate- and lignin-active enzymes (Dataset S1). We hypothesized that organisms should cluster with others of similar nutritional mode, perhaps implying nutritional mode for *B. botryosum* and *J. argillacea*. Fig. 2 shows the wood-decaying fungi plotted on the first two principal components, which together

explain 50% of the variability in the data. For this analysis, we again relied on categorization of fungi as producing either white or brown rot whenever possible. Clear separation of known white- and brown-rotting fungi is seen along PC1. *B. botryosum* and *J. argillacea* group with the white-rot fungi on PC1 and are closest to the model white-rot fungus, *P. chrysosporium*. In contrast, *S. commune* is intermediate between white-rot and brown-rot species along PC1. Both white-rot and brown-rot species are widely distributed along PC2, which suggests heterogeneity in modes of wood degradation within these functional classes. Despite the lack of PODs (Fig. 1), PCA analysis suggests that *B. botryosum* and *J. argillacea* have wood decay properties that are similar to certain white-rot fungi.

Decay Assays in Wood Substrates. To assess the extent to which *B. botryosum* and *J. argillacea* are able to degrade all components of wood, we performed experiments using single-spore isolates of each fungus, on both pine and aspen wood. Both species readily colonized both types of wood, but caused only superficial degradation of the wood surfaces. Nevertheless, in localized areas *B. botryosum* eroded all cell wall layers, indicating degradation and disruption of all cell wall polymers. Hyphae of *B. botryosum* were visible growing in the voids where cell wall degradation had taken place (Fig. 3). The removal of cellulose, hemicellulose, and lignin in these areas is consistent with white rot, whereas in brown rot we would observe residual lignin remaining after a diffuse depolymerization of the cellulose. Similarly, *J. argillacea* degraded a localized area of the wood cells in which all of the cell wall layers were degraded and replaced with the mycelia of the fungus. Once again, complete degradation of all cell wall layers implies all of the wall components have been degraded, as is characteristic of white rot.

We did not include *S. commune* in decay assays as previous studies have shown that this species, although classified as a white-rot species, lacks the ability to degrade lignin appreciably in vitro (55). The *S. commune* genome lacks PODs and has a reduced complement of enzymes bearing cellulose-binding modules (CBM1), but it retains 22 genes encoding LPMOs. Thus, *S. commune* likely has a very different mode of decay than *B. botryosum* and *J. argillacea* (with which it shares the absence of PODs), which is consistent with its isolated position, intermediate between white- and brown-rot species, in the PCA (Fig. 2).

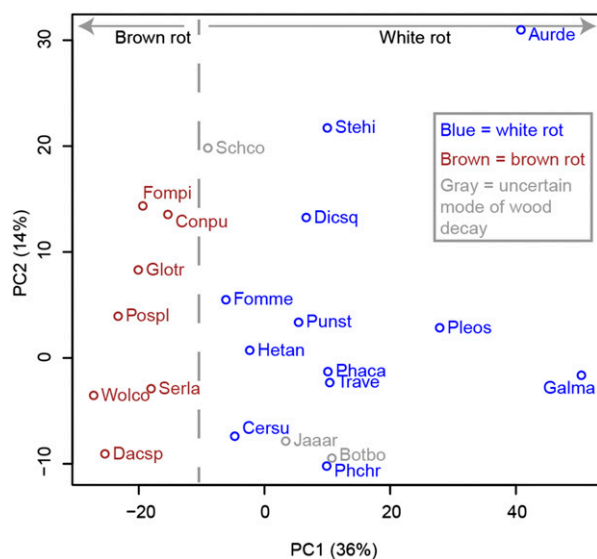


Fig. 2. Wood-decaying basidiomycetes plotted on the first two principal components from phylogenetic PCA of CAZymes (including lignin-related auxiliary activities) of the organisms.

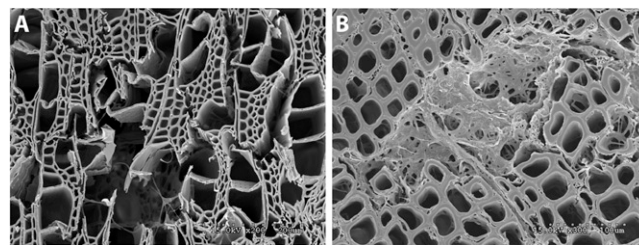


Fig. 3. Wood decay experiments indicating mode of decay by *Botryobasidium botryosum* and *Jaapia argillacea*. (A) Micrograph of *B. botryosum* on aspen wood with vessel, fiber, and parenchyma cell walls degraded. Mycelia are visible growing through the voids. (B) Micrograph of *J. argillacea* on pine showing an area within the wood where the fungus has caused a localized simultaneous decay of the cells. Residual cell wall material and mycelia fill the degraded zone.

Need for a New Classification of Wood Decay Modes. Discussions of the genomic correlates of the white- vs. brown-rot modes of wood decay have typically focused on the lignin-degrading PODs and the hydrolytic and oxidative enzymes involved in attack of crystalline cellulose (17, 23, 25, 72). However, it is also accepted that other enzymes, such as laccases, cellobiose dehydrogenases, and potentially many others, can contribute to white rot (62, 73, 74); accordingly, a database of functional annotations has been dedicated to cataloging lignin-degrading enzymes (49) (Figs. S4 and S5). Our results indicate that the simple dichotomy of white rot vs. brown rot does not adequately reflect the diversity of mechanisms by which wood-rotting fungi obtain nutrition. Specifically, *B. botryosum* and *J. argillacea* show similarities to white-rot fungi in PCA of all predicted carbohydrate- and lignin-active enzymes and can degrade all components of wood, but they do so without the PODs that are a hallmark of white rot. *S. commune* is another putative white-rot fungus (55) that lacks PODs, but it is quite distinct from *B. botryosum* and *J. argillacea* in the PCA (and presumably also in its mode of wood decay). Therefore, we suggest that a more nuanced categorization scheme is needed to describe wood decay by species that degrade all cell wall polymers, including lignin, but lack PODs. As our discovery of the potential role of R-PKSSs in brown rot indicates, other functional considerations beyond lignin-degrading PODs and CAZymes may be important for a biologically descriptive classification of decay modes. Finally, we suggest restricting the term “white rot” to only those fungi that degrade all cell wall polymers through the action of the lignin-degrading PODs in concert with enzymes that attack crystalline cellulose.

Methods

Data Access. Genome assemblies and annotations for the organisms used in this study are available via the JGI Genome Portal MycoCosm (<http://jgi.doe.gov/fungi>; see also Table S1). In addition, the newly sequenced genome assemblies and annotations have been deposited to GenBank under the following accession numbers: *B. botryosum*: AYEP00000000; *G. marginata*: AYUM00000000; *J. argillacea*: AYUL00000000; *P. ostreatus*: AYUK00000000. The versions described in this paper are AYEP01000000, AYUM01000000, AYUL01000000, and AYUK01000000, respectively.

Sequencing, Assembly, and Annotation. The *B. botryosum*, *G. marginata*, and *J. argillacea* genome assemblies were produced using shredded consensus from Velvet-assembled (75) Illumina paired-end data combined with Roche (454) data assembled with Newbler (www.454.com). *P. ostreatus* was sequenced with the Sanger whole-genome shotgun approach and assembled with Arachne (76). All genomes were annotated using the JGI Annotation Pipeline (77), which combines several gene prediction and annotation methods with transcriptomics data, and integrates the annotated genomes into MycoCosm (78), a Web-based fungal resource for comparative analysis.

Protein Sequence Clustering. Predicted protein sequences were clustered using the MCL clustering algorithm (46), with an inflation parameter of 2.0. Two clustering runs were performed: a first one using 63 organisms (33 basidiomycetes, 27 ascomycetes, and 3 from other fungal phyla), which was used for core genes and protein conservation analysis; and a second using 39 organisms (33 basidiomycetes and 4 ascomycetes: *Aspergillus nidulans*, *Pichia stipitis*, *Stagonospora nodorum*, and *Trichoderma reesei*) as outgroups, which was used for generating the phylogenetic tree (see *SI Text* and *Dataset S3* for further details).

Phylogeny. Protein sequences from 183 single-copy clusters were concatenated and multiple-aligned using MAFFT (79) with default parameters, resulting in an alignment with 163,105 amino acid positions. Gblocks (80) was run with the options $t = p$ and $-b4 = 5$ to remove poorly aligned regions, resulting in 38,423 positions. A ML tree was then inferred using RAxML (40) on the Gblocks-trimmed alignment with the PROTGAMMAWAG model, 100 rounds of bootstrapping, and the four Ascomycete organisms *A. nidulans*, *P. stipitis*, *S. nodorum*, and *T. reesei* specified to the program as outgroups. The resulting tree was used for subsequent analyses.

Annotation of Carbohydrate-Active and Auxiliary Redox Enzymes. The carbohydrate-active enzymes (CAZy) and auxiliary redox enzymes (AA) were annotated as in refs. 39 and 49. A manually curated subset of the AA2 family was created, limited to genes predicted to encode high-oxidation potential peroxidases: LiP, MnP, and VP. These are referred to in this work as “POD.”

Annotation of Secondary Metabolism Enzymes. Proteins with an AMP-binding domain (PF00501), a phosphopantetheinyl-binding domain (PF00550), and a condensation domain (PF00668) were designated as NRPS. Proteins with a terpene synthase domain (PF03936) were designated as TS. Proteins with a ketoacyl-synthase (KS) domain (PF00109 and PF02801) were divided into three categories: FAS, NR-PKS, and R-PKS based on their phylogenetic relationships. A gene genealogy was constructed by maximum parsimony analysis in PAUP* 4.0b10 (81) using a ClustalW+ (82) alignment of deduced amino acid sequences. Statistical support for branches was generated by bootstrap analysis with 1,000 pseudoreplications. Putative FASs were grouped in a clade (100% support) that included an Ascomycete KS with significant identity to a FAS from *Aspergillus nidulans* (83). Putative NR-PKSs were grouped in a clade (90% support) that included an Ascomycete NR-PKS involved in the synthesis of a nonreduced polyketide (84). Putative R-PKSs were grouped in three clades (83%, 100%, and 64% support), of which a majority included a ketoreductase (KR) domain (PF08659) (85).

Correlation of Genomic Features and Lifestyle. To infer correlations between genomic features and phenotypes (e.g., repeat content with genome size, or CAZymes with white or brown rot), we used Felsenstein's method of independent contrasts (50) as implemented in the contrast program from Phylip, version 3.62 downloaded from <http://evolution.genetics.washington.edu/phylip> (86).

Phylogenetic PCA. Phylogenetic PCA was implemented using the function *phyl.pca* from the R package *phytools* (www.phytools.org). The algorithm corrects the covariance/correlation matrices for nonindependence among the observations for species, by additionally taking into account the expected covariances/correlations due to pure phylogenetic relatedness of species (71). A matrix of CAZyme gene number in each organism (*Dataset S1*), restricted to the wood decay fungi (Aurde, Botbo, Cersu, Conpu, Dacsq, Discq, Fomme, Fompi, Galma, Glotr, Hetan, Jaaar, Phaca, Phchr, Pleos, Posp, Punst, Schco, Serla, Stehi, Trave, and Wolco), and the ML tree, were used as input.

Wood Decay Assays. Micromorphological observations of degraded aspen (*Populus* sp.) and pine (*Pinus* sp.) wood were used to elucidate the type of decay resulting after inoculation with *B. botryosum* or *J. argillacea*. Physical aspects of decay were investigated using scanning electron microscopy on wood wafers after decay using the same single spore isolate of each fungus that was used for genome sequencing. Dried wood wafers from the sapwood of aspen and pine were cut to $10 \times 10 \times 1$ mm, hydrated to 80–100% moisture, and autoclaved for 60 min at 120 °C. Wood wafers were placed on inoculated Petri plates with malt extract agar (15 g of malt extract, 15 g of agar, 2 g of yeast extract, and 1,000 mL of water). Six plates of each wood type were inoculated with each fungus by placing a 2-mm plug of the assay fungus at the center of a Petri plate 14 d before wafers were added. Wafers were removed 90 d after inoculation and prepared for scanning electron microscopy as previously described (87). Samples were examined and photographed using a Hitachi S3500 N (Hitachi) scanning electron microscope.

Culture Conditions and Enzyme Assays. Standard media included carbon- and nitrogen-starved B3 (88, 89) as well as a more complex medium containing 0.5% (wt/vol) Wiley-mill ground aspen as sole carbon source (90). Culture filtrates were concentrated 6- to 10-fold with 10-kDa spin concentrators (Pall). Protein concentration was determined by the Bradford assay (Sigma-Aldrich). Measurement of LiP, MnP, laccase, and glyoxal oxidase involved oxidation of veratryl alcohol (Sigma-Aldrich) (58), 2,6-dimethoxyphenol (59), 2,2-azonodi-3-ethylbenzothiazoline-6-sulfuric acid (Boehringer), and methyl glyoxal as substrate (91), respectively (see *SI Text* and *Table S4* for further details).

ACKNOWLEDGMENTS. We thank Jill Gaskell (Forest Products Laboratory) for assistance with cultures and enzyme assays. The work conducted by the US Department of Energy (DOE) Joint Genome Institute is supported by the Office of Science of the DOE under Contract DE-AC02-05CH11231. J.D.W. and D.J. were supported by the DOE Great Lakes Bioenergy Research Center (DOE Office of Science Biological and Environmental Research Contract DE-FC02-07ER64494). B.H. is Honorary Professor at the Faculty of Health and Medical Sciences, University of Copenhagen. F.M.'s research group is part of the Laboratory of Excellence for Advanced Research on the Biology of Forest Ecosystems (ANR-11-LABX-0002-01).

- Kirk PMCP, Minter DW, Stalpers JA (2008) *Dictionary of the Fungi* (CAB International, Wallingford, UK), 10th Ed, p 72.
- Johansson M, Stenlid J (1985) Infection of roots of Norway spruce (*Picea abies*) by *Heterobasidion Annosum*: Initial reactions in sapwood by wounding and infection. *Eur J Forest Pathol* 15(1):32–45.
- Otrosina WJ, Chase TE, Cobb FW, Korhonen K (1993) Population structure of *Heterobasidion annosum* from North America and Europe. *Can J Bot* 71(8):1064–1071.
- Martin F, et al. (2008) The genome of *Laccaria bicolor* provides insights into mycorrhizal symbiosis. *Nature* 452(7183):88–92.
- Jin Y, et al. (2007) Characterization of seedling infection types and adult plant infection responses of monogenic Sr gene lines to race TTKS of *Puccinia graminis* f. sp. *tritici*. *Plant Dis* 91(9):1096–1099.
- Jin Y, Wanyera R, Kinyua M, Jin Y, Singh R (2005) The spread of *Puccinia graminis* f. sp. *tritici* with broad virulence in eastern Africa. *Phytopathology* 95(6):549.
- Duplessis S, et al. (2011) Obligate biotrophy features unraveled by the genomic analysis of rust fungi. *Proc Natl Acad Sci USA* 108(22):9166–9171.
- Rihs JD, Padhye AA, Good CB (1996) Brain abscess caused by *Schizophyllum commune*: An emerging basidiomycete pathogen. *J Clin Microbiol* 34(7):1628–1632.
- Lacaz CdaS, Heins-Vaccari EM, De Melo NT, Hernandez-Arriagada GL (1996) Basidiomycosis: A review of the literature. *Rev Inst Med Trop Sao Paulo* 38(5):379–390.
- Brown SM, Campbell LT, Lodge JK (2007) *Cryptococcus neoformans*, a fungus under stress. *Curr Opin Microbiol* 10(4):320–325.
- Dawson TL, Jr. (2007) *Malassezia globosa* and *restricta*: Breakthrough understanding of the etiology and treatment of dandruff and seborrheic dermatitis through whole-genome analysis. *J Invest Dermatol Symp Proc* 12(2):15–19.
- Morin E, et al. (2012) Genome sequence of the button mushroom *Agaricus bisporus* reveals mechanisms governing adaptation to a humic-rich ecological niche. *Proc Natl Acad Sci USA* 109(43):17501–17506.
- Ohm RA, et al. (2010) Genome sequence of the model mushroom *Schizophyllum commune*. *Nat Biotechnol* 28(9):957–963.
- Stajich JE, et al. (2010) Insights into evolution of multicellular fungi from the assembled chromosomes of the mushroom *Coprinopsis cinerea* (*Coprinus cinereus*). *Proc Natl Acad Sci USA* 107(26):11889–11894.
- Griffith NT, Barnett HL (1967) Mycoparasitism by Basidiomycetes in culture. *Mycologia* 59(1):149–154.
- Padamsee M, et al. (2012) The genome of the xerotolerant mold *Walleria sebi* reveals adaptations to osmotic stress and suggests cryptic sexual reproduction. *Fungal Genet Biol* 49(3):217–226.
- Floudas D, et al. (2012) The Paleozoic origin of enzymatic lignin decomposition reconstructed from 31 fungal genomes. *Science* 336(6089):1715–1719.
- Benson DA, Karsch-Mizrachi I, Lipman DJ, Ostell J, Sayers EW (2009) GenBank. *Nucleic Acids Res* 37(Database issue):D26–D31.
- Sayers EW, et al. (2009) Database resources of the National Center for Biotechnology Information. *Nucleic Acids Res* 37(Database issue):D5–D15.
- Eastwood DC, et al. (2011) The plant cell wall-decomposing machinery underlies the functional diversity of forest fungi. *Science* 333(6043):762–765.
- Fernandez-Fueyo E, et al. (2012) Comparative genomics of *Ceriporiopsis subvermisporea* and *Phanerochaete chrysosporium* provide insight into selective ligninolysis. *Proc Natl Acad Sci USA* 109(14):5458–5463, and correction (2012) 109(21):8352.
- Martinez D, et al. (2009) Genome, transcriptome, and secretome analysis of wood decay fungus *Postia placenta* supports unique mechanisms of lignocellulose conversion. *Proc Natl Acad Sci USA* 106(6):1954–1959.
- Martinez D, et al. (2004) Genome sequence of the lignocellulose degrading fungus *Phanerochaete chrysosporium* strain RP78. *Nat Biotechnol* 22(6):695–700.
- Baldrian P, Valášková V (2008) Degradation of cellulose by basidiomycetous fungi. *FEMS Microbiol Rev* 32(3):501–521.

25. Lundell TK, Mäkelä MR, Hildén K (2010) Lignin-modifying enzymes in filamentous basidiomycetes—ecological, functional and phylogenetic review. *J Basic Microbiol* 50(1):5–20.
26. Morita T, Fukuoka T, Imura T, Kitamoto D (2009) Production of glycolipid biosurfactants by basidiomycetous yeasts. *Biotechnol Appl Biochem* 53(Pt 1):39–49.
27. Rasmussen ML, Shrestha P, Khanal SK, Pometto AL, 3rd, Hans van Leeuwen J (2010) Sequential saccharification of corn fiber and ethanol production by the brown rot fungus *Gloeophyllum trabeum*. *Bioresour Technol* 101(10):3526–3533.
28. Grigoriev IV, et al. (2011) Fueling the future with fungal genomics. *Mycology* 2(3): 192–209.
29. Daniel G (1994) Use of electron microscopy for aiding our understanding of wood biodegradation. *FEMS Microbiol Rev* 13:199–233.
30. Blanchette R (1991) Delignification by wood-decay fungi. *Annu Rev Phytopathol* 29:381–398.
31. Eriksson K-EL, Blanchette RA, Ander P (1990) *Microbial and Enzymatic Degradation of Wood and Wood Components* (Springer, Berlin).
32. Blanchette R (1995) Degradation of the lignocellulose complex in wood. *Can J Bot* 73(Suppl 1):999–1010.
33. Worrall JJ, Anagnost SE, Zabel RA (1997) Comparison of wood decay among diverse lignicolous fungi. *Mycologia* 89:199–219.
34. Yelle DJ, Ralph J, Lu F, Hammel KE (2008) Evidence for cleavage of lignin by a brown rot basidiomycete. *Environ Microbiol* 10(7):1844–1849.
35. Niemenmaa O, Uusi-Rauva A, Hatakka A (2008) Demethoxylation of [O¹⁴CH₃]-labelled lignin model compounds by the brown-rot fungi *Gloeophyllum trabeum* and *Poria (Postia) placenta*. *Biodegradation* 19(4):555–565.
36. Kirk TK, Farrell RL (1987) Enzymatic “combustion”: The microbial degradation of lignin. *Annu Rev Microbiol* 41:465–505.
37. Hammel KE, Cullen D (2008) Role of fungal peroxidases in biological ligninolysis. *Curr Opin Plant Biol* 11(3):349–355.
38. Martinez AT (2002) Molecular biology and structure-function of lignin-degrading heme peroxidases. *Enzyme Microb Technol* 30:425–444.
39. Lombard V, Golaconda Ramulu H, Drula E, Coutinho PM, Henrissat B (2014) The carbohydrate-active enzymes database (CAZy) in 2013. *Nucleic Acids Res* 42(Database issue):D490–D495.
40. Stamatakis A (2006) RAxML-VI-HPC: Maximum likelihood-based phylogenetic analyses with thousands of taxa and mixed models. *Bioinformatics* 22(21):2688–2690.
41. Matheny PB, et al. (2007) Contributions of rpb2 and tef1 to the phylogeny of mushrooms and allies (Basidiomycota, Fungi). *Mol Phylogenet Evol* 43(2):430–451.
42. Binder M, Larsson KH, Matheny PB, Hibbett DS (2010) Amylocorticiales ord. nov. and Jaapiales ord. nov.: Early diverging clades of agaricomycetidae dominated by corticioid forms. *Mycologia* 102(4):865–880.
43. Hibbett DS (2006) A phylogenetic overview of the Agaricomycotina. *Mycologia* 98(6): 917–925.
44. Hibbett DS, et al. (2007) A higher-level phylogenetic classification of the Fungi. *Mycol Res* 111(Pt 5):509–547.
45. Matheny PB, Gossmann JA, Zalar P, Kumar TKA, Hibbett DS (2006) Resolving the phylogenetic position of the Wallemiomycetes: An enigmatic major lineage of Basidiomycota. *Can J Bot* 84(12):1794–1805.
46. Enright AJ, Van Dongen S, Ouzounis CA (2002) An efficient algorithm for large-scale detection of protein families. *Nucleic Acids Res* 30(7):1575–1584.
47. Altschul SF, Gish W, Miller W, Myers EW, Lipman DJ (1990) Basic local alignment search tool. *J Mol Biol* 215(3):403–410.
48. Koonin EV, et al. (2004) A comprehensive evolutionary classification of proteins encoded in complete eukaryotic genomes. *Genome Biol* 5(2):R7.
49. Levasseur A, Drula E, Lombard V, Coutinho PM, Henrissat B (2013) Expansion of the enzymatic repertoire of the CAZy database to integrate auxiliary redox enzymes. *Biootechnol Biofuels* 6(1):41.
50. Felsenstein J (1985) Phylogenies and the comparative method. *Am Nat* 125(1):1–15.
51. Harris PV, et al. (2010) Stimulation of lignocellulosic biomass hydrolysis by proteins of glycoside hydrolase family 61: Structure and function of a large, enigmatic family. *Biochemistry* 49(15):3305–3316.
52. Langston JA, et al. (2011) Oxidoreductive cellulose depolymerization by the enzymes cellulase dehydrogenase and glycoside hydrolase 61. *Appl Environ Microbiol* 77(19): 7007–7015.
53. Quinlan RJ, et al. (2011) Insights into the oxidative degradation of cellulose by a copper metalloenzyme that exploits biomass components. *Proc Natl Acad Sci USA* 108(37):15079–15084.
54. Vaaje-Kolstad G, et al. (2010) An oxidative enzyme boosting the enzymatic conversion of recalcitrant polysaccharides. *Science* 330(6001):219–222.
55. Schmidt O, Liese W (1980) Variability of wood degrading enzymes of *Schizophyllum commune*. *Holzforschung* 34(2):67–72.
56. Blodig W, et al. (1998) Autocatalytic formation of a hydroxy group at C beta of trp171 in lignin peroxidase. *Biochemistry* 37(25):8832–8838.
57. Poulos TL, Edwards SL, Wariishi H, Gold MH (1993) Crystallographic refinement of lignin peroxidase at 2 Å. *J Biol Chem* 268(6):4429–4440.
58. Tien M, Kirk TK (1984) Lignin-degrading enzyme from *Phanerochaete chrysosporium*: Purification, characterization, and catalytic properties of a unique H₂O₂-requiring oxygenase. *Proc Natl Acad Sci USA* 81(8):2280–2284.
59. Wariishi H, Valli K, Gold MH (1992) Manganese(II) oxidation by manganese peroxidase from the basidiomycete *Phanerochaete chrysosporium*. Kinetic mechanism and role of chelators. *J Biol Chem* 267(33):23688–23695.
60. Kerem Z, Hammel KE (1999) Biodegradative mechanism of the brown rot basidiomycete *Gloeophyllum trabeum*: Evidence for an extracellular hydroquinone-driven Fenton reaction. *FEBS Lett* 446(1):49–54.
61. Jensen KA, Jr., Houtman CJ, Ryan ZC, Hammel KE (2001) Pathways for extracellular Fenton chemistry in the brown rot basidiomycete *Gloeophyllum trabeum*. *Appl Environ Microbiol* 67(6):2705–2711.
62. Eggert C, Temp U, Eriksson KEL (1996) The ligninolytic system of the white rot fungus *Pycnoporus cinnabarinus*: Purification and characterization of the laccase. *Appl Environ Microbiol* 62(4):1151–1158.
63. Niku-Paavola ML, Karhunen E, Salola P, Raunio V (1988) Ligninolytic enzymes of the white-rot fungus *Phlebia radiata*. *Biochem J* 254(3):877–883.
64. Keller NP, Turner G, Bennett JW (2005) Fungal secondary metabolism—from biochemistry to genomics. *Nat Rev Microbiol* 3(12):937–947.
65. Arantes V, Milagres AM, Filley TR, Goodell B (2011) Lignocellulosic polysaccharides and lignin degradation by wood decay fungi: The relevance of nonenzymatic Fenton-based reactions. *J Ind Microbiol Biotechnol* 38(4):541–555.
66. Cohen R, Jensen KA, Houtman CJ, Hammel KE (2002) Significant levels of extracellular reactive oxygen species produced by brown rot basidiomycetes on cellulose. *FEBS Lett* 531(3):483–488.
67. Korripally P, Timokhin VI, Houtman CJ, Mozuch MD, Hammel KE (2013) Evidence from *Serpula lacrymans* that 2,5-dimethoxyhydroquinone is a lignocellulolytic agent of divergent brown rot basidiomycetes. *Appl Environ Microbiol* 79(7):2377–2383.
68. Shimokawa T, Nakamura M, Hayashi N, Ishihara M (2004) Production of 2,5-dimethoxyhydroquinone by the brown-rot fungus *Serpula lacrymans* to drive extracellular Fenton reaction. *Holzforschung* 58:305–310.
69. Lackner G, Misiek M, Braesel J, Hoffmeister D (2012) Genome mining reveals the evolutionary origin and biosynthetic potential of basidiomycete polyketide synthases. *Fungal Genet Biol* 49(12):996–1003.
70. Wawrzyn GT, Quin MB, Choudhary S, López-Gallego F, Schmidt-Dannert C (2012) Draft genome of *Omphalotus olearius* provides a predictive framework for sesquiterpenoid natural product biosynthesis in Basidiomycota. *Chem Biol* 19(6):772–783.
71. Revell LJ (2009) Size-correction and principal components for interspecific comparative studies. *Evolution* 63(12):3258–3268.
72. Gold MH, Alic M (1993) Molecular biology of the lignin-degrading basidiomycete *Phanerochaete chrysosporium*. *Microbiol Rev* 57(3):605–622.
73. Ander P, Eriksson KE (1976) Importance of phenol oxidase activity in lignin degradation by white-rot fungus *Sporotrichum pulverulentum*. *Arch Microbiol* 109(1-2): 1–8.
74. Hiroi T, Eriksson KE (1976) Microbiological degradation of lignin: Influence of cellulose on degradation of lignins by white-rot fungus *Pleurotus ostreatus*. *Sven Papperstidn* 79(5):157–161.
75. Zerbino DR, Birney E (2008) Velvet: Algorithms for de novo short read assembly using de Bruijn graphs. *Genome Res* 18(5):821–829.
76. Jaffe DB, et al. (2003) Whole-genome sequence assembly for mammalian genomes: Arachne 2. *Genome Res* 13(1):91–96.
77. Grigoriev IV, Martinez DA, Salamov AA (2006) Fungal genomic annotation. *Appl Mycol Biotechnol* 6:123–142.
78. Grigoriev IV, et al. (2014) MycoCosm portal: Gearing up for 1000 fungal genomes. *Nucleic Acids Res* 42(Database issue):D699–704.
79. Katoh K, Misawa K, Kuma K, Miyata T (2002) MAFFT: A novel method for rapid multiple sequence alignment based on fast Fourier transform. *Nucleic Acids Res* 30(14):3059–3066.
80. Castresana J (2000) Selection of conserved blocks from multiple alignments for their use in phylogenetic analysis. *Mol Biol Evol* 17(4):540–552.
81. Swofford DL (2003) *PAUP*. Phylogenetic Analysis Using Parsimony (*and Other Methods). Version 4* (Sinauer Associates, Sunderland, MA).
82. Larkin MA, et al. (2007) Clustal W and Clustal X version 2.0. *Bioinformatics* 23(21): 2947–2948.
83. Brown DW, Adams TH, Keller NP (1996) *Aspergillus* has distinct fatty acid synthases for primary and secondary metabolism. *Proc Natl Acad Sci USA* 93(25):14873–14877.
84. Li Y, Chooi YH, Sheng Y, Valentine JS, Tang Y (2011) Comparative characterization of fungal anthracenone and naphthacenedione biosynthetic pathways reveals an α -hydroxylation-dependent Claisen-like cyclization catalyzed by a dimanganese thioesterase. *J Am Chem Soc* 133(39):15773–15785.
85. Hopwood DA, Sherman DH (1990) Molecular genetics of polyketides and its comparison to fatty acid biosynthesis. *Annu Rev Genet* 24:37–66.
86. Felsenstein J (2005) PHYLIP (Phylogeny Inference Package) Distributed by the author. (Department of Genome Sciences, University of Washington, Seattle), Version 3.6.
87. Blanchette RA, et al. (2010) An Antarctic hot spot for fungi at Shackleton's historic hut on Cape Royds. *Microb Ecol* 60(1):29–38.
88. Brown A, Sims PFG, Raeder U, Broda P (1988) Multiple ligninase-related genes from *Phanerochaete chrysosporium*. *Gene* 73(1):77–85.
89. Kirk TK, Schultz E, Connors WJ, Lorentz LF, Zeikus JG (1978) Influence of culture parameters on lignin metabolism by *Phanerochaete chrysosporium*. *Arch Microbiol* 117: 277–285.
90. Hori C, et al. (2013) Genomewide analysis of polysaccharides degrading enzymes in 11 white- and brown-rot Polyporales provides insight into mechanisms of wood decay. *Mycologia* 105(6):1412–1427.
91. Kersten PJ, Kirk TK (1987) Involvement of a new enzyme, glyoxal oxidase, in extracellular H₂O₂ production by *Phanerochaete chrysosporium*. *J Bacteriol* 169(5):2195–2201.

Supporting Information

Riley et al. 10.1073/pnas.1400592111

SI Text

Genome Annotation

Before gene prediction, assembly scaffolds were masked using RepeatMasker (1), RepBase library (2), and most frequent (>150 times) repeats recognized by RepeatScout (3). The following combination of gene predictors was run on the masked assembly: ab initio Fgenesh (4) and GeneMark (5), homology-based Fgenesh+ (4) and Genewise (6) seeded by BLASTx (7) alignments against National Center for Biotechnology Information (NCBI) NR database, and transcriptome-based assemblies. In addition to protein-coding genes, tRNAs were predicted using tRNAscan-SE (8). All predicted proteins are functionally annotated using SignalP (9) for signal sequences, TMHMM (10) for transmembrane domains, InterProScan (11) for integrated collection of functional and structure protein domains, and protein alignments to NCBI nr, SwissProt (www.expasy.org/sprot/), KEGG (12) for metabolic pathways, and KOG (13) for eukaryotic clusters of orthologs. Interpro and SwissProt hits are used to map Gene Ontology (GO) terms (14). For each genomic locus, the best representative gene model was selected based on a combination of protein homology and EST support, which resulted in the final set of 6,903 gene models used for further analysis in this work.

Genomes Overview

Genome sizes vary over an order of magnitude in Basidiomycota (Fig. S1 and Table S1). The plant-pathogenic rusts (15) *Puccinia graminis* (88.6 Mb) and *Melampsora laricis-populina* (101.1 Mb), along with the early-diverging Agaricomycete *Auricularia delicata* (16) (74.9 Mb) feature the largest genomes, whereas the human pathogen *Malassezia globosa* (17) (9.0 Mb) and xerophilic mold *Wallemia sebi* (18) (9.8 Mb) have the smallest genomes.

Protein Clusters and Phylogeny

Gene families in 33 basidiomycetes and 30 other fungi (Table S2) with sequenced genomes were inferred by Markov chain (MCL) clustering (19) of all-vs.-all protein BLAST (7) alignments. Two clustering runs were performed. The first clustering run, used for core genes and conservation analysis, used 765,862 protein sequences resulting in 121,327 clusters and is visible at the following: <http://genome.jgi-psf.org/clustering/pages/cluster/clusters.jsf?runId=2655>. The second run, used for building the phylogenetic tree, used 472,010 protein sequences resulting in 73,519 clusters, and is visible at the following: <http://genome.jgi-psf.org/clustering/pages/cluster/clusters.jsf?runId=2656>. From this second cluster run, 183 clusters, in which each organism contributed a single protein sequence, were extracted for subsequent use in inferring the phylogeny. (Dataset S3 contains one cluster per line, with each protein in a cluster denoted by its Joint Genome Institute (JGI) protein id and JGI portal id separated by the “|” symbol).

The maximum-likelihood phylogeny (20), inferred from the protein sequences of 183 conserved gene families, along with an overview of genome size, repeat content, gene number, and gene conservation is shown in Fig. S1. The earliest-diverging nodes of the Agaricomycetes remain unclear, in particular the position of *Piriformospora indica* (Sebacinales) and the position of *Jaapia argillacea* (Jaapiales). The former species was inferred as monophyletic with *Auricularia delicata*, whereas previous multigene phylogenies (21–24) placed them in different clades along the backbone of the Agaricomycetes. The position of the Jaapiales is likewise somewhat uncertain; it forms a well-supported clade with *Gloeophyllum trabeum* and *Punctularia strigosozonata*, but that clade's

position on the tree, either as a sister clade of the Polyporales, or of the clade containing the Russulales, Boletales, and Agaricales, is uncertain.

The protein clusters' KOG (13) annotations suggest that one-half of the proteins in Basidiomycota have no predicted function (Fig. S2). However, only 8% of the proteins in the “core proteome” (i.e., MCL clusters that have at least one member in all Basidiomycota) have no KOG annotation, suggesting we can predict functions for some 92% of the core proteins. In contrast, 78% of “noncore” proteins (those present in some, but not all basidiomycetes) have no KOG annotation. Protein families sporadically present in basidiomycetes are therefore mostly of unknown function and may provide clues to the unique adaptations of basidiomycete lineages.

Secondary Metabolism

Phylogenetic relationships of Basidiomycete and Ascomycete polyketide synthases (PKSs) within and among species were examined by maximum parsimony analysis of deduced amino acid sequences of 225 keto synthase (KS) domains (PF00109.17 and PF02801.13) identified in 35 Basidiomycete (the 33 used in the rest of this analysis plus *Rhodotorula graminis* and *Sporobolomyces roseus* downloaded from MycoCosm: <http://jgi.doe.gov/fungi>) and four Ascomycete genomes (*Aspergillus niger*, *Pichia stipitis*, *Stagonospora nodorum*, and *Trichoderma reesei*). The KS from the *Gallus gallus* fatty acid synthase (FAS) served as an outgroup. AA sequence alignments were generated with the ClustalW (25) using the Blosum multiple sequence alignment scoring matrix (26). The aligned sequences were then used to construct a gene genealogy using parsimony in PAUP* 4.0b10 (27). Statistical support for branches was generated by bootstrap analysis with 1,000 pseudoreplications.

To investigate the secondary metabolite biosynthetic potential of the Basidiomycetes, we examined the evolution of the KS domain, a key domain involved in polyketide and fatty acid synthesis, from the predicted protein sequence of 144 KS domains from 35 Basidiomycetes and 81 KS domains from four Ascomycetes. Maximum parsimony analysis of the amino acid alignment resolved the predicted peptides into five major groups (Fig. S3) corresponding to FASs, nonreducing type PKSs (NR-PKSs), and reducing type PKSs (R-PKSs) and is consistent with previous work (28–30).

BLASTP analysis against the NCBI NR database with KSs, represented by the dark blue and light blue triangles in Fig. S3, match numerous yeast and fungal FASs ($E < 1 \times 10^{-100}$), suggesting that the query proteins are involved in the synthesis of a fully reduced carbon chain typical of constitutive fatty acid biosynthesis. The largest clade (large dark blue triangle), with 79% bootstrap support, includes 38 KS domains from 34 different Basidiomycetes (Fig. S3, large blue triangle). Most Basidiomycetes possess one FAS gene; four Basidiomycetes have two FASs, whereas one, *Malassezia globosa*, lacks a FAS. *M. globosa* is associated with most skin disease in humans, including dandruff, and presumably does not need a FAS as it uses fatty acids present in sebaceous gland secretions (31). The clade with one KS from each Ascomycete examined in this study (small dark blue triangle), likely represents constitutive FASs. Three branches, represented by light blue triangles, include five KSs from two Ascomycetes; four from *A. niger* and one from *S. nodorum*. Products from these FAS-like proteins have not yet been determined. Adjacent to the FAS branches is a branch with three Ascomycete KSs (dark pink triangle), with 99% support, that by BLASTP, are similar

to the keto acyl synthases or type III PKSs involved in secondary metabolite synthesis in *Aspergillus* species (32).

Domains adjacent to the KS domain present in the “PKS and PKS-like” group are typically found in nonribosomal peptide synthetases (NRPSs). In contrast to most previously described PKSs with an NRPS module in Ascomycetes, the NRPS domain (s) here are located at the amino terminus rather than the carboxyl terminus. The first group (green) includes three Basidiomycete KS domains, which, in each case, is adjacent to a condensation (C) (PF00668.11), AMP-binding (PF00501.19), and phosphopantetheine-binding (PP-binding) (PF00550.16) domain. The next group (gray), with 83% bootstrap support, includes 14 Basidiomycete KSs present in three sister clades, each with 100% bootstrap support. The domain organization of the predicted proteins associated with each clade is significantly different but consistent within each clade. For example, the predicted proteins in the first clade include an AMP-binding domain adjacent to the KS followed by an acyl transferase (AT) (PF00698.12) and a keto reductase (KR) (PF08659.1) domain. In contrast, most of the predicted proteins in the second clade include an AMP-binding domain adjacent to the KS but lack AT and KR domains, whereas the predicted proteins in the third clade lack the AMP-binding domain but have an epimerase domain (PF01370.12) before the AT domain and lack a KR domain. The observation that five of the six fungi with KSs in this clade are white-rot fungi may suggest that the chemical product(s) generated may be important for a subset of fungi with this lifestyle, despite their distant relatedness. Adjacent to the “PKS and PKS-like group” is a branch (light pink) with two Ascomycete KSs, which BLASTP analysis suggest are homologs of 6-methylsalicylic acid synthase from *Penicillium griseofulvum* ($E = 1 \times 10^{-154}$).

The NR-PKS group consists of 48 KSs from both Basidiomycetes and Ascomycetes in a single clade with 90% bootstrap support. A majority of the Basidiomycetes KSs (26) forms a clade that is sister to a clade, with 93% support, composed of both Basidiomycete (4) and Ascomycete (10) KSs. The remaining seven Ascomycete KSs belong to a more basal clade, with 82% support. Of the 27 KSs in the Basidiomycete clade, two pairs of KSs have 100% bootstrap support, which may reflect recent gene duplication events. The 27 KSs are very well distributed with 87% of white-rot and 71% brown-rot fungi having at least one member. This group also appears to be ancient as only a few branches have significant bootstrap support.

The KSs corresponding to R-PKSs separate into two major groups corresponding to their phylum. For example, all 49 Ascomycetes KSs, representing the three previously described R-PKS clades I, II, and III (28–30), form one group, whereas the 58 Basidiomycete KSs form the other group. The limited number of orthologous gene pairs in the Ascomycete set was previously noted for a much larger KS set and it was suggested that recent gene duplication events have not contributed significantly to the expansion of this gene family (28, 29). The 58 KSs from 19 Basidiomycetes form two sister clades with 100% (42 KSs) and 64% (16 KSs) bootstrap support. Most of the KSs of this group (96%) are from wood-decaying fungi. In contrast to the Ascomycete R-PKSs noted above, nine pairs of KSs from the same fungus share between 64% and 100% bootstrap support (average, 91%), suggesting that gene duplication events contributed more significantly to PKS the expansion of this gene family. Analysis of additional, more closely related Basidiomycete genomes may suggest how long in the evolutionary past these events occurred.

Clustering of Auxiliary Redox Enzymes

The AA families of auxiliary redox enzymes are thought to break down cell wall components, including lignin (33). To better understand the role of these enzymes in wood-decaying basidiomycetes, we used the CAFE program (34) to explore their evolution according to a stochastic model of gene death and birth. Additionally,

we performed hierarchical clustering of both AA families and organisms, using a table of the number of genes in each family. As done elsewhere in this study, we used a manually curated subset of the AA2 family, limited to the predicted high-oxidation potential peroxidases (PODs): lignin peroxidase (LiP), manganese peroxidase (MnP), and versatile peroxidase (VP). We refer to this subset as “POD.”

The CAFE analysis revealed POD, AA3_2 (GMC oxidoreductase), and AA9 [lytic polysaccharide monoxygenase (LPMO)] as significantly departing from a random model of gene birth and death, using a family-wide significance threshold of 0.05, implying lineage-specific shifts of the duplication and loss of these genes, presumably in accordance with lifestyle. The CAFE analysis also allowed the inference of statistically significant gene family gains and losses in the various lineages. Fig. S4 shows a heat map of the number of genes in each AA family for each organism, along with the number of genes inferred to be gained or lost since that organism's split with its nearest neighbor. It is clear that the POD, AA3_2, and AA9 families have generally undergone gains in the white-rot lineages and losses in the brown-rot, mycorrhizal, and soil saprotrophic lineages, consistent with an earlier report (16). Interestingly, *Botryobasidium botryosum*, *J. argillacea* have substantial gains in the AA9 family, and *Schizophyllum commune* is also rich in these enzymes, suggesting a possible heightened importance of oxidative attack on cellulose in fungi that lack ligninolytic PODs, but that nevertheless are capable of degrading all cell wall components. *S. commune* also has undergone reductions in the AA1_1 (laccase) and AA5_1 (copper radical oxidase) families, which are abundant in white-rot lineages, and which therefore highlight *S. commune*'s break from the white-rot/brown-rot dichotomy.

The results of the double-hierarchical clustering based on AA families shown in Fig. S5 is in full agreement with previous results based on the analysis of a different set of fungal genomes (33). Thus, families AA1_1, AA3_2, AA3_3, POD, and AA5_1 cluster together in Fig. S5 in accord with the known cooperation of these enzymes (33). A difference between the results of Levasseur et al. (33) and the analysis reported here is that our clustering also includes LPMOs, whereas Levasseur et al. focused exclusively on ligninolytic enzymes. Interestingly, family AA9 LPMOs clustered with families AA1_1, AA3_2, AA3_3, POD, and AA5_1, suggesting a certain degree of cooperation of the set of enzyme families during the breakdown of plant cell walls.

In an analysis based exclusively on the ligninolytic machinery, Levasseur et al. unexpectedly found *S. commune* in the BR group. Here, we show that the addition of family AA9 LPMOs to the oxidoreductase gene sets used for the clustering is sufficient to take *S. commune* out of the BR group and to place this fungus near *B. botryosum*. *J. argillacea* is most similar to white-rot fungus *A. delicata*.

Assays for Oxidoreductases Related to Degradation of Lignin

Three media were evaluated. Carbon-limited B3 and nitrogen-limited B3 medium (35, 36) were incubated statically for 5, 9, and 11 d. Cultures were flushed with O₂ after 2 d. Nutrient-starved B3 media have been widely used for production of LiP, MnP, and glyoxal oxidase. A more complex medium contained 0.5% (wt/vol) Wiley-mill ground *Populus grandidentata* (aspen) as sole carbon source in Highley's basal salts (37). These cultures were incubated on a rotary shaker at 150 rpm. In all cases, 20 mL of medium was inoculated with mycelium-covered agar plugs. *Phanerochaete chrysosporium* was incubated at 37 °C, and all other cultures remained at room temperature (~20 °C). Based on appearance and total extracellular protein, white-rot fungi *P. chrysosporium*, *Ceriporiopsis subvermispora* and brown-rot fungi *Wolfiporia cocos* and *Postia placenta* grew at the expected rates and were therefore harvested at day 5. The sequenced *Jaapia*

argillacea MUCL-33604 SS and *Botryobasidium botryosum* FD172 SS-1 monokaryons exhibited relatively slower growth, so additional cultures were harvested after 9- and 11-d incubation.

Cultures were harvested by filtration through Miracloth (Calbiochem). The B3 culture filtrates were then passed through a 0.45- μ m filter before concentration 6- to 10-fold with a 10-kDa cutoff Microsep spin concentrator (Pall). Filtrates from cultures containing ground *Populus* required a low-speed centrifugation before the 0.45- μ m filter and Microsep concentration.

Protein concentration was determined by the Bradford assay (Sigma-Aldrich) according manufacturer's instructions. Measurement of MnP activity was based on the oxidative dimerization of 2,6-dimethoxyphenol (2,6-DMP) (38). The reaction mixture contained 100 μ M 2,6-DMP, 100 μ M MnSO₄, 50 mM sodium tartrate (pH 4.5), 50 μ M H₂O₂, and culture filtrate in 1,000 μ L. LiP activity was determined by conversion of veratryl alcohol (Sigma-Aldrich) to veratraldehyde in the presence of H₂O₂ (39). Fifty millimolar sodium tartrate (pH 3.0) served as buffer and the culture filtrate

was mixed with 2 mM veratryl alcohol and 0.4 mM H₂O₂ in 1,000 μ L at room temperature. Laccase (Lac) activity was assayed with 2,2'-azobodi-3-ethylbenzothiazoline-6-sulfuric acid (ABTS) (Boehringer) as a substrate in 30 mM glycine/HCl buffer (pH 3.0) at room temperature (40). The reaction contained 14 μ M ABTS and culture filtrate in 1,000 μ L. Copper radical oxidase activity was measured as optimized for glyoxal oxidase (GLOX) using methylglyoxal as substrate (41).

As expected, we observed MnP and LiP activity after 5 d in B3 cultures inoculated with the white-rot fungi *P. chrysosporium* and *C. subvermispora* (Table S4). Also consistent with many earlier studies, methylglyoxal oxidation was highest in *P. chrysosporium* cultures, likely due to GLOX. ABTS oxidation indicated laccase activity in *C. subvermispora* in B3 media. Consistent with the absence of PODs, veratryl alcohol and DMP oxidation could not be detected in the *J. argillacea* or *B. botryosum* culture filtrates. ABTS oxidation, typical of laccase activity, was also absent despite the presence of a laccase-encoding gene in the *B. botryosum* genome.

- Smit AFA, Hubley R, Green P (1996–2010) RepeatMasker Open-3.0. Available at www.repeatmasker.org. Accessed November 2002.
- Jurka J, et al. (2005) Repbase Update, a database of eukaryotic repetitive elements. *Cytogenet Genome Res* 110(1-4):462–467.
- Price AL, Jones NC, Pevzner PA (2005) De novo identification of repeat families in large genomes. *Bioinformatics* 21(Suppl 1):i351–i358.
- Salamov AA, Solovyev VV (2000) *Ab initio* gene finding in *Drosophila* genomic DNA. *Genome Res* 10(4):516–522.
- Ter-Hovhannissyan V, Lomsadze A, Chernoff YO, Borodovsky M (2008) Gene prediction in novel fungal genomes using an *ab initio* algorithm with unsupervised training. *Genome Res* 18(12):1979–1990.
- Birney E, Clamp M, Durbin R (2004) GeneWise and Genomewise. *Genome Res* 14(5):988–995.
- Altschul SF, Gish W, Miller W, Myers EW, Lipman DJ (1990) Basic local alignment search tool. *J Mol Biol* 215(3):403–410.
- Lowe TM, Eddy SR (1997) tRNAscan-SE: A program for improved detection of transfer RNA genes in genomic sequence. *Nucleic Acids Res* 25(5):955–964.
- Nielsen H, Engelbrecht J, Brunak S, von Heijne G (1997) Identification of prokaryotic and eukaryotic signal peptides and prediction of their cleavage sites. *Protein Eng* 10(1):1–6.
- Melén K, Krogh A, von Heijne G (2003) Reliability measures for membrane protein topology prediction algorithms. *J Mol Biol* 327(3):735–744.
- Quevillon E, et al. (2005) InterProScan: Protein domains identifier. *Nucleic Acids Res* 33(Web Server issue):W116–W120.
- Kanehisa M, et al. (2006) From genomics to chemical genomics: New developments in KEGG. *Nucleic Acids Res* 34(Database issue):D354–D357.
- Koonin EV, et al. (2004) A comprehensive evolutionary classification of proteins encoded in complete eukaryotic genomes. *Genome Biol* 5(2):R7.
- Ashburner M, et al.; The Gene Ontology Consortium (2000) Gene ontology: Tool for the unification of biology. *Nat Genet* 25(1):25–29.
- Duplessis S, et al. (2011) Obligate biotrophy features unraveled by the genomic analysis of rust fungi. *Proc Natl Acad Sci USA* 108(22):9166–9171.
- Floudas D, et al. (2012) The Paleozoic origin of enzymatic lignin decomposition reconstructed from 31 fungal genomes. *Science* 336(6089):1715–1719.
- Xu J, et al. (2007) Dandruff-associated *Malassezia* genomes reveal convergent and divergent virulence traits shared with plant and human fungal pathogens. *Proc Natl Acad Sci USA* 104(47):18730–18735.
- Padamsee M, et al. (2012) The genome of the xerotolerant mold *Wallemia sebi* reveals adaptations to osmotic stress and suggests cryptic sexual reproduction. *Fungal Genet Biol* 49(3):217–226.
- Enright AJ, Van Dongen S, Ouzounis CA (2002) An efficient algorithm for large-scale detection of protein families. *Nucleic Acids Res* 30(7):1575–1584.
- Stamatakis A (2006) RAxML-VI-HPC: Maximum likelihood-based phylogenetic analyses with thousands of taxa and mixed models. *Bioinformatics* 22(21):2688–2690.
- Hibbett DS (2006) A phylogenetic overview of the Agaricomycotina. *Mycologia* 98(6):917–925.
- Matheny PB, Gossman JA, Zalar P, Kumar TKA, Hibbett DS (2006) Resolving the phylogenetic position of the Wallemiomycetes: An enigmatic major lineage of Basidiomycota. *Can J Bot* 84(12):1794–1805.
- Matheny PB, et al. (2007) Contributions of *rpb2* and *tef1* to the phylogeny of mushrooms and allies (Basidiomycota, Fungi). *Mol Phylogenet Evol* 43(2):430–451.
- Hibbett DS, et al. (2007) A higher-level phylogenetic classification of the Fungi. *Mycol Res* 111(Pt 5):509–547.
- Larkin MA, et al. (2007) Clustal W and Clustal X version 2.0. *Bioinformatics* 23(21):2947–2948.
- Henikoff S, Henikoff JG (1992) Amino acid substitution matrices from protein blocks. *Proc Natl Acad Sci USA* 89(22):10915–10919.
- Swofford DL (2003) *PAUP*. Phylogenetic Analysis Using Parsimony (*and Other Methods). Version 4* (Sinauer Associates, Sunderland, MA).
- Kroken S, Glass NL, Taylor JW, Yoder OC, Turgeon BG (2003) Phylogenomic analysis of type I polyketide synthase genes in pathogenic and saprobic ascomycetes. *Proc Natl Acad Sci USA* 100(26):15670–15675.
- Baker SE, et al. (2006) Two polyketide synthase-encoding genes are required for biosynthesis of the polyketide virulence factor, T-toxin, by *Cochliobolus heterostrophus*. *Mol Plant Microbe Interact* 19(2):139–149.
- Brown DW, Butchko RA, Baker SE, Proctor RH (2012) Phylogenomic and functional domain analysis of polyketide synthases in *Fusarium*. *Fungal Biol* 116(2):318–331.
- Dawson TL, Jr. (2007) *Malassezia globosa* and *restricta*: Breakthrough understanding of the etiology and treatment of dandruff and seborrheic dermatitis through whole-genome analysis. *J Invest Dermatol Symp Proc* 12(2):15–19.
- Seshime Y, Juvvadi PR, Kitamoto K, Ebizuka Y, Fujii I (2010) Identification of csypyrone B1 as the novel product of *Aspergillus oryzae* type III polyketide synthase CsyB. *Bioorg Med Chem* 18(12):4542–4546.
- Levasseur A, Drula E, Lombard V, Coutinho PM, Henrissat B (2013) Expansion of the enzymatic repertoire of the CAZy database to integrate auxiliary redox enzymes. *Biotechnol Biofuels* 6(1):41.
- De Bie T, Cristianini N, Demuth JP, Hahn MW (2006) CAFE: A computational tool for the study of gene family evolution. *Bioinformatics* 22(10):1269–1271.
- Brown A, Sims PFG, Raeder U, Broda P (1988) Multiple ligninase-related genes from *Phanerochaete chrysosporium*. *Gene* 73(1):77–85.
- Kirk TK, Schultz E, Connors WJ, Lorentz LF, Zeikus JG (1978) Influence of culture parameters on lignin metabolism by *Phanerochaete chrysosporium*. *Arch Microbiol* 117:277–285.
- Hori C, et al. (2013) Genomewide analysis of polysaccharides degrading enzymes in 11 white- and brown-rot Polyporales provides insight into mechanisms of wood decay. *Mycologia* 105(6):1412–1427.
- Wariishi H, Valli K, Gold MH (1992) Manganese(II) oxidation by manganese peroxidase from the basidiomycete *Phanerochaete chrysosporium*. Kinetic mechanism and role of chelators. *J Biol Chem* 267(33):23688–23695.
- Tien M, Kirk TK (1984) Lignin-degrading enzyme from *Phanerochaete chrysosporium*: Purification, characterization, and catalytic properties of a unique H₂O₂-requiring oxygenase. *Proc Natl Acad Sci USA* 81(8):2280–2284.
- Niku-Paavola ML, Karhunen E, Salola P, Raunio V (1988) Ligninolytic enzymes of the white-rot fungus *Phlebia radiata*. *Biochem J* 254(3):877–883.
- Kersten PJ, Kirk TK (1987) Involvement of a new enzyme, glyoxal oxidase, in extracellular H₂O₂ production by *Phanerochaete chrysosporium*. *J Bacteriol* 169(5):2195–2201.

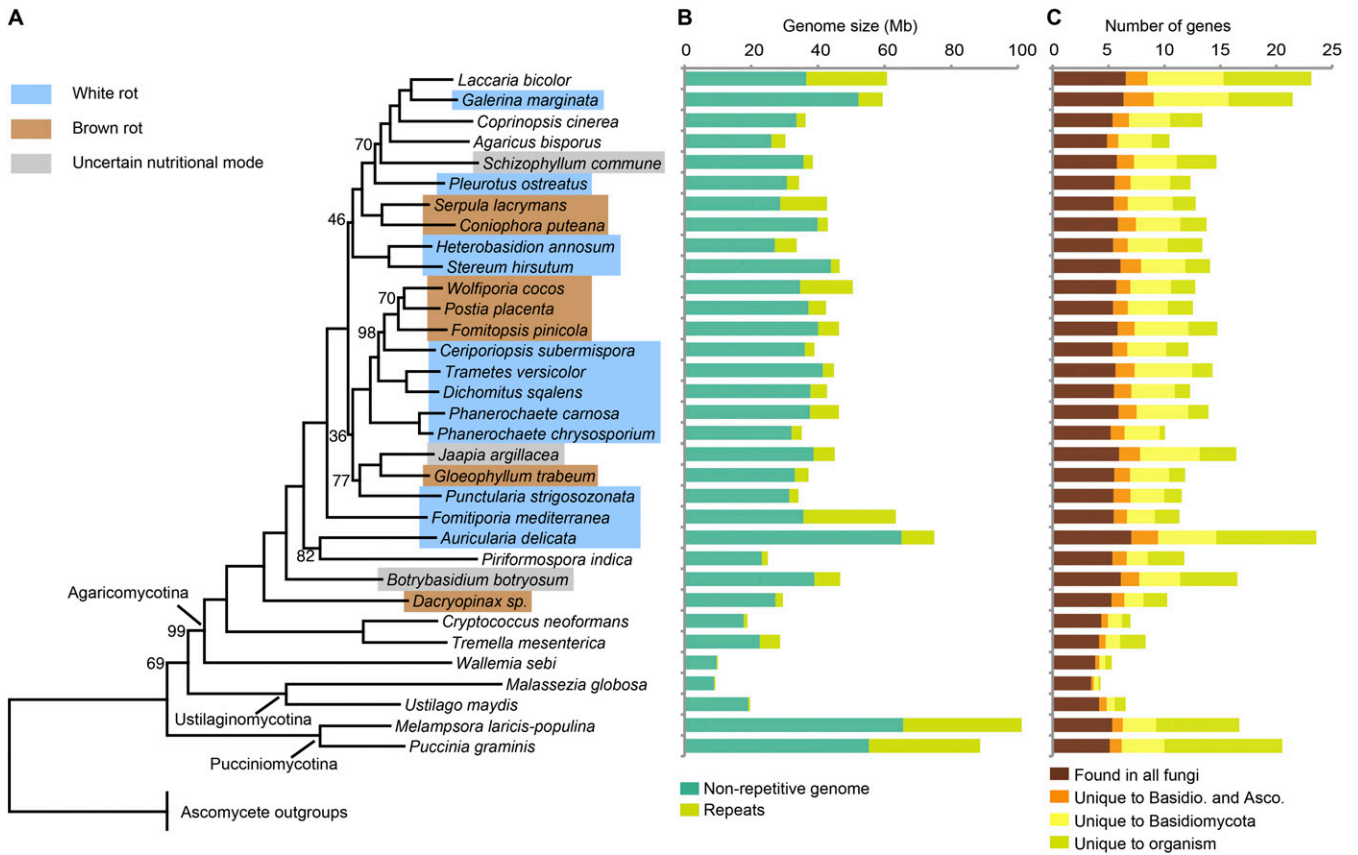


Fig. S1. Phylogeny, genome size and repeats, and gene conservation among basidiomycetes. (A) Maximum-likelihood tree of 33 basidiomycetes based on concatenated alignments of 183 widely conserved genes. Ascomycete outgroups are omitted from the figure. Bootstrap values of branches are 100% except where indicated. (B) Repeat content in basidiomycetes is highly variant, ranging from 1% to 44%. (C) Conservation of genes in basidiomycetes.

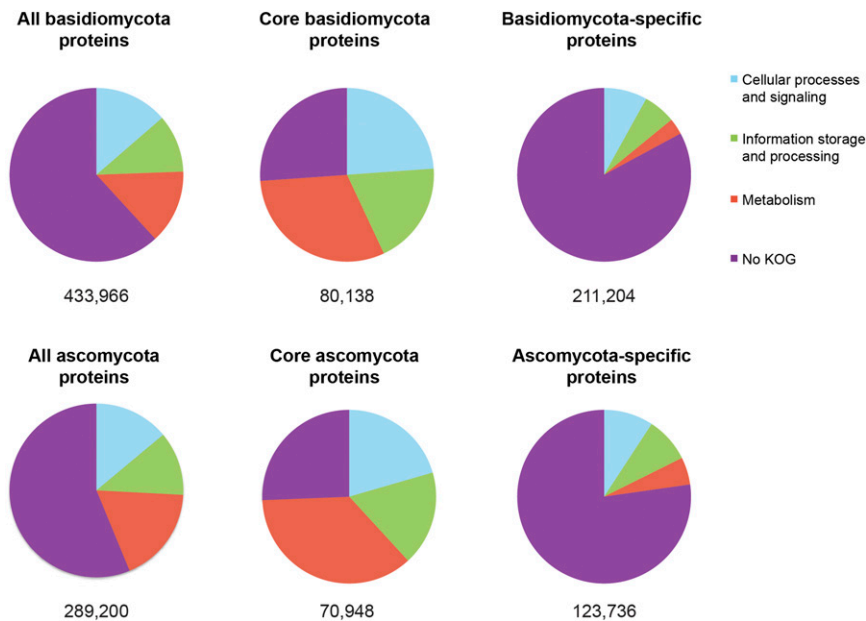


Fig. S2. Core genes of Basidiomycota. Notice that one-half of basidiomycete proteins have no KOG annotation (function unknown); 92% of core basidiomycete proteins have a KOG annotation (putative function predicted); and 78% of noncore basidiomycete proteins have no KOG annotation (function unknown).

Table S2. Nonbasidiomycete fungi used for comparative purposes

Subkingdom	Phylum	Subphylum	Organism	JGI portal ID		
Dikarya	Ascomycota	Pezizomycotina	<i>Stagonospora nodorum</i> SN15	Stano2		
			<i>Aspergillus niger</i> ATCC 1015	Aspni5		
			<i>Aspergillus nidulans</i>	Aspnid1		
			<i>Botrytis cinerea</i>	Botci1		
			<i>Fusarium graminearum</i>	Fusgr1		
			<i>Fusarium oxysporum</i>	Fusox1		
			<i>Leptosphaeria maculans</i>	Lepmu1		
			<i>Magnaporthe grisea</i>	Maggr1		
			<i>Mycosphaerella graminicola</i>	Mycgr3		
			<i>Nectria hematococca</i>	Necha2		
			<i>Neurospora crassa</i> OR74A	Neucr1		
			<i>Neurospora tetrasperma</i> FGSC 2508 mat A	Neute_matA2		
			<i>Neurospora tetrasperma</i> FGSC 2509 mat a	Neute_mat_a1		
			<i>Pyrenophora tritici-repentis</i>	Pyrr1		
			<i>Pyrenophora teres f. teres</i>	Pyrrt1		
			<i>Sclerotinia sclerotiorum</i>	Scpsc1		
			<i>Sporotrichum thermophile</i>	Spoth2		
			<i>Thielavia terrestris</i>	Thite2		
			<i>Trichoderma atroviride</i>	Triat2		
			<i>Trichoderma reesei</i>	Trire2		
		<i>Tuber melanosporum</i>	Tubme1			
		<i>Verticillium dahliae</i>	Verda1			
		Saccharomycotina	<i>Candida tenuis</i> NRRL Y-1498	Cante1		
			<i>Dekkera bruxellensis</i> CBS 2499	Dekbr2		
			<i>Pichia stipitis</i>	Picst3		
			<i>Saccharomyces cerevisiae</i> S288C	Sacce1		
			<i>Spathaspora passalidarum</i> NRRL Y-27907	Spapa3		
			<i>Batrachochytrium dendrobatidis</i> JAM81	Batde5		
		Fungi incertae sedis	Chytridiomycota	N/A		
				Mucoromycotina		
Mucoromycotina	<i>Phycomyces blakesleeianus</i> NRRL1555		Phybl2			
		<i>Rhizopus oryzae</i> 99-880	Rhior3			

